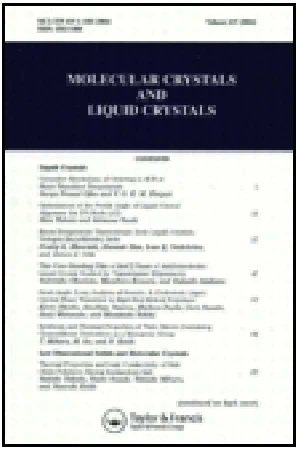

Molecular Crystals and Liquid Crystals

Liquid Crystal Beam Deflector with a Photopolymer Prism

Jae-Hong Park [a] & Iam Choon Khoo [a]

[a] Department of Electrical Engineering, Pennsylvania State University, University Park, Pennsylvania, USA

Version of record first published: 22 Sep 2006

To cite this article: Jae-Hong Park & Iam Choon Khoo (2006): Liquid Crystal Beam Deflector with a Photopolymer Prism, Molecular Crystals and Liquid Crystals, 454:1, 135/[537]-143/[545]

To link to this article: http://dx.doi.org/10.1080/15421400600654280

Mol. Cryst. Liq. Cryst., Vol. 454, pp. 135/[537]–143/[545], 2006
Copyright © Taylor & Francis Group, LLC
ISSN: 1542-1406 print/1563-5287 online
DOI: 10.1080/15421400600654280

Liquid Crystal Beam Deflector with a Photopolymer Prism

Jae-Hong Park
Iam Choon Khoo
Department of Electrical Engineering, Pennsylvania State University,
University Park, Pennsylvania, USA

Liquid crystal (LC) beam deflector with a photopolymer prism is presented. The polymer surface relief is produced by ultraviolet (UV) exposure and serves as an optical prism. The method for producing this polymer prism is based on the diffusion process of pre-polymer which occurs under inhomogeneous UV exposure. We can obtain a tunable deflecting angle by injecting LC into the cell with the polymer prism formed on one surface of it. Our deflecting device gives complete single-order diffraction and a controllable steering over ~1° with an applied ac voltage of 5 V.

Keywords: beam steering; deflector; liquid crystal; photopolymer; surface relief

INTRODUCTION

A photopolymer is a material having repeated molecules linked to each other [1]. When this photopolymer material is introduced inside of the LC cell, the resultant composite system enables new interesting physical phenomena. Such system has attracted great interest in recent years because of its potential for use in optic devices [2–5] or novel displays [6]. In this paper, we propose an LC deflector with a photopolymer wedge capable of electrically controlled beam steering. The underlying operational mechanism is based on the polarization separation and the voltage dependence of the deflecting angle produced by a

The work is supported in parts by the Army Research Office and The Air Force Office of Scientific Research. One of the authors (JHP) acknowledges the Information and Communication National Scholarship Program of the Ministry of Information and Communication of the Republic of Korea.

Address correspondence to Iam Choon Khoo, Department of Electrical Engineering, Pennsylvania State University, University Park, PA 16802, USA. E-mail: ick1@psu.edu

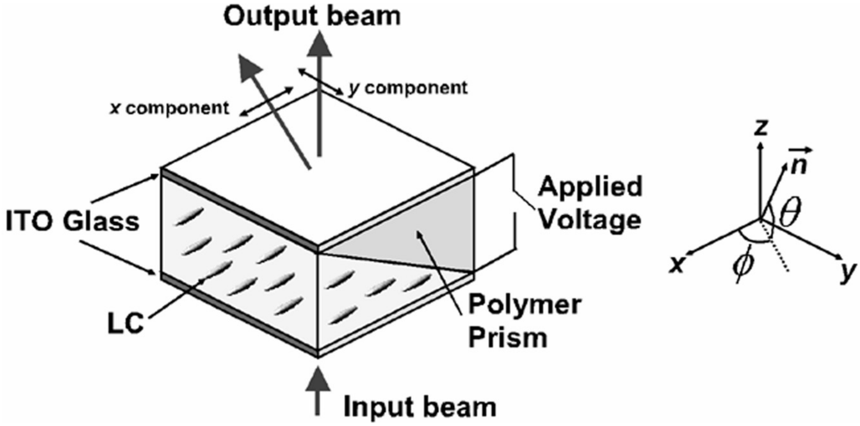

FIGURE 1 The schematic diagram of the LC deflector with a photopolymer prism and the coordinate system.

dielectric wedge structure. The schematic diagram of our device is illustrated in Figure 1. It consists of two indium tin oxide (ITO) glass substrates. The polymer prism is formed on the one surface of them. In our device scheme, LC is aligned along the x axis and the ordinary refractive index of LC is almost identical to the refractive index of the polymer. The input beam is passing through the z direction and linearly polarized in the xy plain. Any linearly polarized state of an input beam can be decomposed into two orthogonal linearly polarized states. Therefore, the y component of the input beam perpendicular to the molecular director do not experience any phase difference, whereas the x component experiences the refractive index change and provides the steering capability.

EXPERIMENTAL

For fabricating the polymer prism, a photocurable prepolymer, NOA65 of Norland products was used. The refractive index n_P and the dielectric constant ε_P of the cured NOA65 are 1.524 at 633 nm and 4.6 at 1 kHz. This photopolymer layer was irradiated by the ultraviolet (UV) light generated from a UV lamp (Model 22-UV Lasercraft Inc.) at a distance of 1 cm for 10 minutes through a photomask (Fig. 2(a)) with a linear aperture of 1 mm in width. The photomask is then removed and the sample was illuminated with the same UV power for 20 minutes for full photocrosslinking of the polymer. When the polymer is illuminated through the photomask, the photopolymerization process begins at the position corresponding to the aperture. Then, the difference in pre-polymer

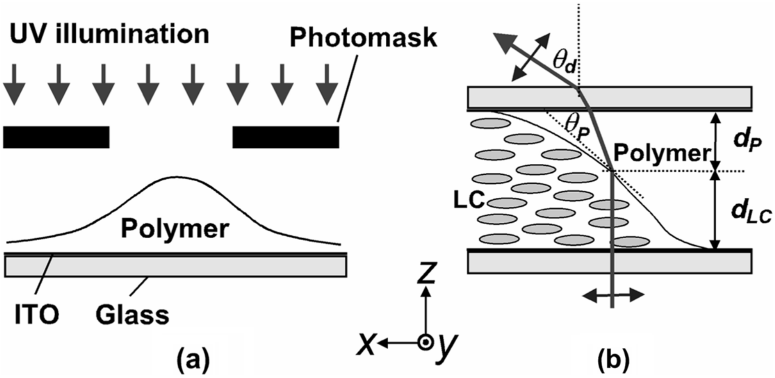

FIGURE 2 (a) The fabrication process for the polymer prism and (b) the schematic diagram of the LC deflector with the polymer prism.

density between the illuminated area and the unilluminated one causes prepolymer to diffuse into the illuminated region to join the polymerization process. As a result, the polymer relief is formed after full photopolymerization. This polymer relief acts as an optical prism. We defined the maximum wedge angle in the one side of the polymer as the wedge angle θ_P (Fig. 2(b)) and calculated it from the deflecting angle of an incident beam before cell fabrication. This wedge angle θ_P depends on many parameters such as the diffusion/reaction constants of the polymer, the polymer layer thickness, the aperture size and the UV power. In our case, we fixed all above conditions and varied the wedge angle by controlling the UV illumination time. As the illumination time increases, the wedge angle θ_P increases and saturates. In our case, the wedge angle saturates at ~12 minutes illumination with photomask and the corresponding maximum wedge angle was ~5°. The polyvinyl alcohol (PVA) alignment layer was spin-coated onto this cured polymer surface and was rubbed unidirectionally to produce uniform homogeneous alignment. The sample cell was assembled with the above prepared substrate and the other with only the PVA layer. We used 10 μm glass spacers to maintain the cell gap. The nematic LC used for this study is a commercial nematic LC E7 of E. Merck. The ordinary and extraordinary refractive indices of it at room temperature are $n_o = 1.518$ and $n_e = 1.737$, respectively, at 633 nm. The dielectric constants at 1 kHz and the elastic constants are $\varepsilon_{||} = 18.96$, $\varepsilon_{\perp} = 5.15$, $K_1 = 11.2 \times 10^{-12}$ N, $K_2 = 6.8 \times 10^{-12}$ N and $K_3 = 18.6 \times 10^{-12}$ N, respectively [7]. A low-power (1 mW) linearly polarized He-Ne laser of 632.8 nm in wavelength was used for this study. The angle between the rubbing direction (the x direction) and the input polarizer was varied from 0° to 90°. To minimize the effect of the nonuniform slope of the polymer wedge, we put a lens of 100 mm focal length with a focal spot of ~200 μm diameter in front of the sample cell. The deflecting angle was measured as a function of the applied voltage. All of the measurements were performed using a square wave voltage of 1 kHz at room temperature.

NUMERICAL SIMULATION

For numerical simulation, a one-dimensional model is considered for simplicity. When we set the coordinate axes as shown in Figure 1 and LC is aligned along the x axis in both surfaces, the director of LC is expressed as follows.

$$\vec{n} = \left(n_x, n_y, n_z\right) = (\cos\theta, 0, \sin\theta), \tag{1}$$

where the θ is the tilt angle measured from the surface toward the z-axis. In order to determine the orientation of LC, the Ossen-Frank strain free energy was used as follows.

$$F = \frac{1}{2}K_1(\nabla\cdot\vec{n})^2 + \frac{1}{2}K_2(\vec{n}\cdot\nabla\times\vec{n})^2 + \frac{1}{2}K_3(\vec{n}\times\nabla\times\vec{n})^2 - \frac{1}{2}\vec{E}\cdot\overset{\leftrightarrow}{\varepsilon}\cdot\vec{E}, \tag{2}$$

where $\vec{n}$ is the unit director of LC, K_1, K_2, K_3 are the elastic constants, $\vec{E}$ is the electic field vector and $\overset{\leftrightarrow}{\varepsilon}$ is the dielectric tensor, respectively. After an initial state is set in the cell, the director field of LC is deformed by the interaction between the electric field and dielectric anisotropy of the LC, which creates a deformation of the director. This deformation increases the above elastic energy which is minimized by following Euler-Lagrange equation.

$$\gamma\frac{\partial n_i}{\partial t} = \frac{d}{dz}\left(\frac{\partial F}{\partial(dn_i/dz)}\right) - \frac{\partial F}{\partial n_i}, \qquad i = x, y, z. \tag{3}$$

In calculating the electric potential at the LC/polymer interface, we utilize the fact that the normal components of the electric displacement, $D_z = \varepsilon_{zz}E_z$, must be continuous at the interface. We used relaxation method to calculate the director profile. From the calculated director profiles $\theta(z)$, we can obtain the effective refractive index of LC n_{LC} as follows.

$$n_{LC} = \frac{n_o n_e}{d}\int_0^d \left(n_e^2\sin^2\theta(z) + n_o^2\cos^2\theta(z)\right)^{-1/2} dz, \tag{4}$$

In the presence of an applied voltage V, the director profiles can be calculated as a function of the applied voltage and the resultant refractive index of LC is varied.

As shown in Figure 2(b), the deflecting angle θ_d can be defined and measured as a function of the applied voltage. Assuming the PVA layer and ITO are coated on both substrates homogeneously with the same thickness, the deflecting angle θ_d is given by

$$\theta_d = \sin^{-1}(n_p \sin(\sin^{-1}(n_{LC}/n_P \sin\theta_P) - \theta_P)), \tag{5}$$

where n_{LC} and n_P are the effective LC and the polymer indices of refraction, and θ_P is the polymer wedge angle, respectively. A relatively large LC index of refraction n_{LC} and a large polymer wedge angle θ_P are desirable to obtain the larger deflecting angle θ_d as shown in Figure 3.

Figure 4(a) shows the deflecting angle variation as a function of the applied voltage for LC E7 and polymer NOA65. In this simulation, the polymer thickness was not considered for simplicity. As expected, the deflecting angle can be controlled by the applied voltage with a different maximum angle depending on the polymer wedge angle. Basically, n_{LC} is a function of the polarization of the input beam and the effective voltage across the LC V_{LC} is given by

$$V_{LC} = V_a\left(1 + \frac{d_P/d_{LC}}{\varepsilon_P/\varepsilon_{LC}}\right)^{-1}, \tag{6}$$

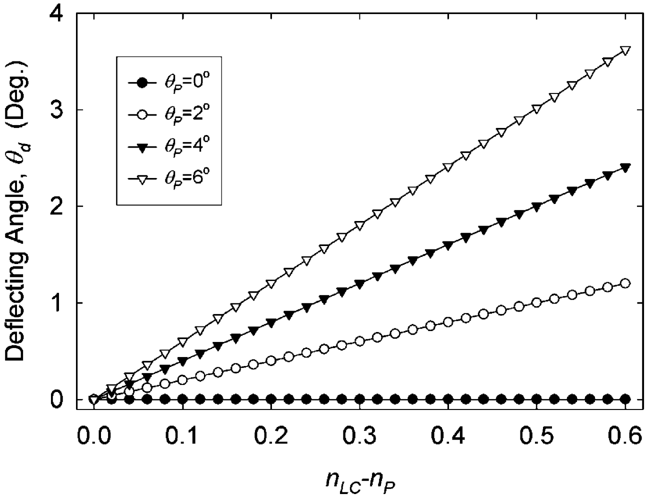

FIGURE 3 The deflecting angle change as a function of refractive index difference between LC and polymer under various polymer wedge angles. $n_P = 1.524$ was used for this calculation.

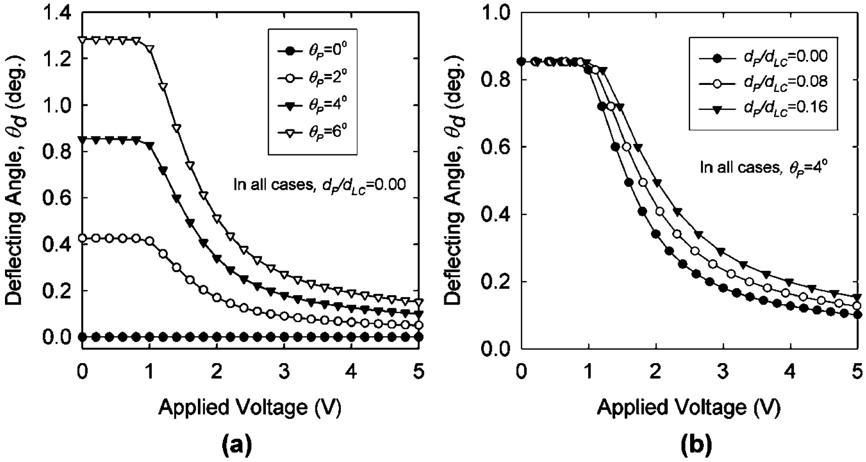

FIGURE 4 (a) The deflecting angle as a function of the applied voltage for various polymer wedge angles and (b) for various layer thickness.

where V_a is an externally applied voltage, d's are the thickness of each layer, and ε's are the dielectric constants. The scaled dielectric constant and the scaled thickness of the polymer with respect to those of the LC layer at the spot where the input beam passes through are the main factors that determine the operating voltage for LC reorientation. As shown in Figure 4(b), the operating voltage increases as the thickness of the polymer layer increases. From the results of the deflecting angle change, we can conclude that it is desirable to have a small value of d_p/d_{LC} to lower the operation voltage of our LC device.

RESULTS

Figure 5 shows the positional change of the deflected beam at the various applied voltage for three input polarizations. When the incident polarization is parallel to the LC director (Fig. 5(a)), the incident beam experiences the extraordinary refractive index of the LC in the absence of an applied voltage. This gives the maximal difference between the refractive index of the LC and that of the polymer so that the resultant deflecting angle has its largest value. As the applied voltage increases, LC molecules become reoriented along the field and the input beam sees a component of ordinary refractive index of the LC resulting in the decreased deflecting angle. On the other hand, when the incident polarization is perpendicular to the LC director as shown

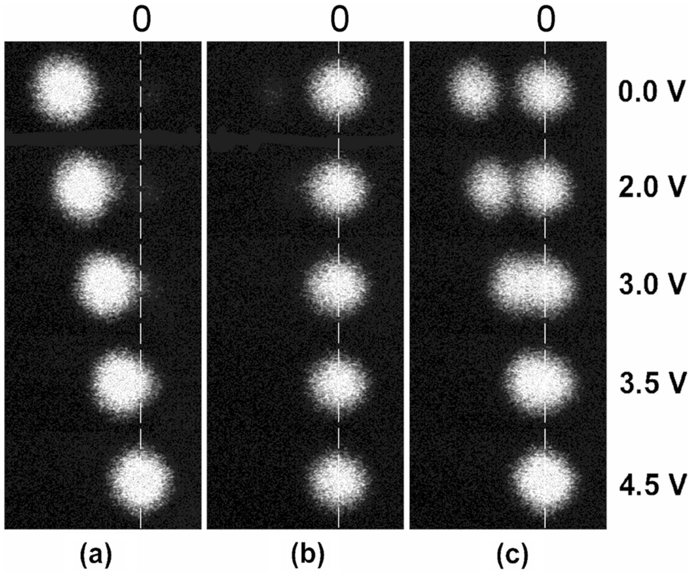

FIGURE 5 The locations of the deflected beam at the various applied voltages in case of (a) an angle of 0° between the rubbing direction and the input polarizer, (b) an angle of 90°, and (c) an angle of 45°, respectively. The '0' denotes the non deflected position.

in Figure 5(b), the incident beam experiences nearly no change of the refractive index at any applied field. As a result, the deflecting angle is not changed even though a high field is applied into the cell. Figure 5(c) shows the deflecting results when the x and y components of the input beam are identical. Clearly, the polarization separation is observed under the low voltage and each component shows its unique behavior as described in Figures 5(a) and (b). This means that under a certain voltage, this device behaves as a polarization beam splitter which separates the arbitrary polarization of input beam into two linear polarizations that are orthogonal to each other.

Figure 6 shows the essential features of our sample device. Here, the electrically changed deflecting characteristics are described. As discussed above, the y component is quite insensitive to the applied voltage V_a while the x component shows strong voltage dependence. For numerical simulations, the scaled dielectric constant $d_P/d_{LC} \sim 0.2$ was found by observing the Fredericks threshold voltage [8] and the polymer wedge angle $\theta_P = 4.3^\circ$ was experimentally measured before cell fabrication. As shown in Figure 6, the simulation results describe well the characteristics of the experimental data such as

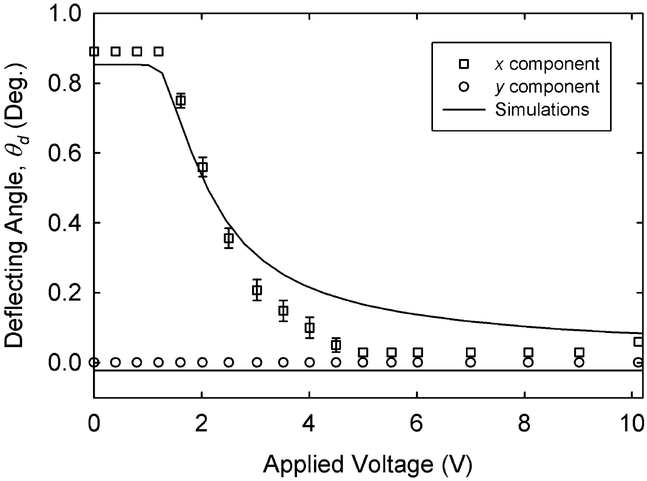

FIGURE 6 Dependence of the deflecting angle as a function of the applied voltage. The open symbols and the solid lines denote the experimental data and the simulation results, respectively.

the polarization separation and the overall behavior of the deflecting angle as a function of the applied voltage. However, there are the mismatch between the simulation data and the measured ones in high voltage regime (3 ~ 10 V). We guess that the nonuniform tilt angle distribution of LC molecules across the sample cell causes this result. It shoud be noted that a large deflecting angle, in principle, can be achieved using the LC with a large refractive index and the polymer with a large wedge angle. In order to increase the polymer wedge angle, one could try to use the photomask with a narrow aperture and irradiate it by a high power UV. If possible, the improved photopolymer with a large diffusion constant could be used.

Let us evaluate the possible application using our device. The optical transmission of the x component of the input beam at various applied voltages were shown in Figure 7. For the measurements, the pin-hole was placed behind the sample device and the optical intensity behind the pin-hole was measured at various applied voltage. It was set to obtain the maximum intensity at the zero voltage. The radius of the input beam and the pin-hole was ~5 mm, respectively and the distance between our LC cell and the pin-hole was ~0.32 m. It is clear that there exists a voltage threshold at which the optical intensity starts being reduced. Since the optical intensity can be controlled electrically, it can be used for the optical attenuator.

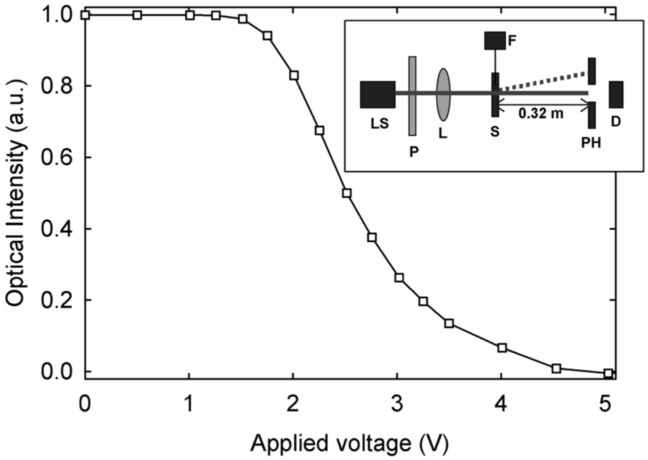

FIGURE 7 The measured optical intensity as a function of the applied voltage. Inset: the schematics of the optical set-up. (LS: laser, P: polarizer, L: lens, S: sample, F: function generator, PH: pin-hole, and D: detector.)

SUMMARY

In summary, we have demonstrated a LC beam deflector using the photopolymer prism. The photopolymer prism was fabricated by UV illumination through the photomask without any chemical etching process. This device enables the polarization separation of an input beam and provides the beam steering capability by the applied voltage. The LC beam steering device presented here can be applied to the optoelectronic systems which need 100% deflected efficiency with the small angle change.

REFERENCES

[1] Gedde, U. W. (1995). *Polymer Physics*, Chapman & Hall: London.
[2] Choi, Y., Park, J.-H., Kim, J.-H., & Lee, S.-D. (2002). *Opt. Mat.*, *21*, 643.
[3] Ji, H.-S., Kim, J.-H., & Kumar, S. (2003). *Opt. Lett.*, *28*, 1147.
[4] Ren, H., Fan, Y.-H., & Wu, S.-T. (2003). *Appl. Phys. Lett.*, *82*, 3168.
[5] Park, J.-H., Khoo, I. C., Yu, C.-J., Jung, M.-S., & Lee, S.-D. (2005). *Appl. Phys. Lett.*, *86*, 021906.
[6] Park, J.-H., Yoon, T.-Y., Lee, W.-J., & Lee, S.-D. (2002). *Mol. Cryst. Liq. Cryst.*, *375*, 433.
[7] Raynes, E. P., Brown, C. V., & Stömer, J. F. (2003). *Appl. Phys. Lett.*, *82*, 13.
[8] Park, J.-H., Kim, S.-J., Jung, M.-S., & Lee, S.-D. (2004). *Mat. Sci. Eng. C*, *24*, 53.